

Supporting Information

Active Phase Distribution Changes within a Catalyst Particle during Fischer-Tropsch Synthesis as revealed by Multi-scale Microscopy

Korneel H. Cats, Joy C. Andrews, Odile Stéphan, Katia March, Chithra Karunakaran, Florian Meirer, Frank M.F. de Groot and Bert M. Weckhuysen

1. X-ray Diffraction

X-ray diffractograms were measured on a Bruker-AXS D2 X-ray diffractometer using Co K_{α} radiation ($\lambda = 1.789 \text{ \AA}$). The diffractograms for the fresh and the spent catalyst are shown in Figure S1. In the fresh catalyst sample only peaks due to TiO_2 and Co_3O_4 are found. Scherrer analysis of the peaks belonging to Co_3O_4 indicates an average crystallite size of about 18 nm. In the spent catalyst we find only peaks caused by TiO_2 and by metallic Co. The particle size of Co was determined to be 10 nm. The discrepancy with the STXM data (where only CoO or CoTiO_3 was found in the spectra) can be explained because a passivation layer of CoO forms around the Co nanoparticles. However, this layer is probably not crystalline. Hence no diffraction peaks belonging to CoO are found. This also explains why the particles appear to be slightly larger in the STEM-EELS experiments.

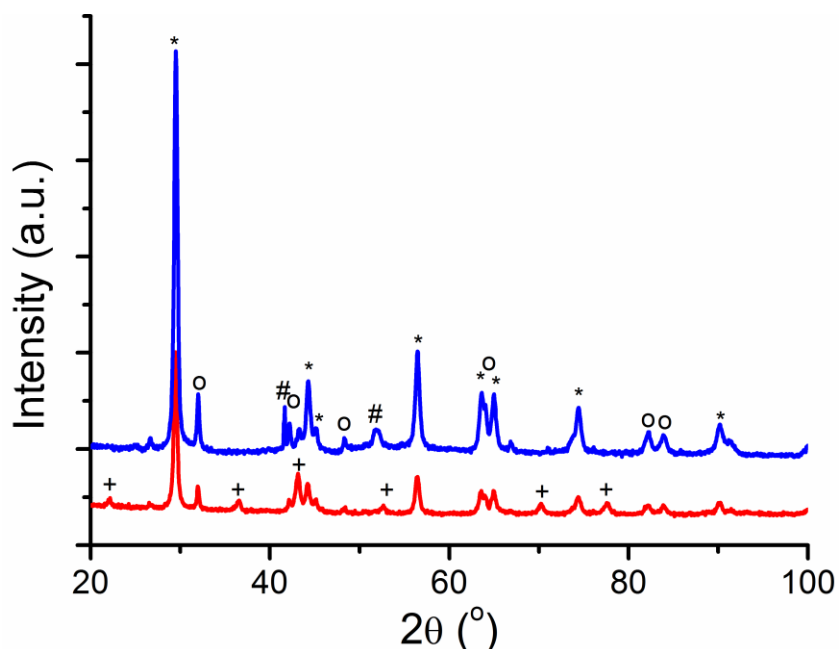


Figure S1: X-ray diffractogram for the fresh (red) and the spent Co/TiO_2 FTS catalysts (blue). Diffraction peaks caused by TiO_2 are marked with '*' (anatase) and "o" (rutile). Diffraction peaks due to Co_3O_4 are marked with '+', and peaks due to metallic Co are marked with '#'.
* * * * *
o o o o o

+ + + + +

2. Soft X-ray Absorption Spectra of CoO and CoTiO_3

The soft X-ray absorption spectra of CoO and CoTiO_3 reference materials at the Co L_3 edge are shown in Figure S2. The spectra are very similar, making the distinction between the two materials based on their soft X-ray spectra impossible.

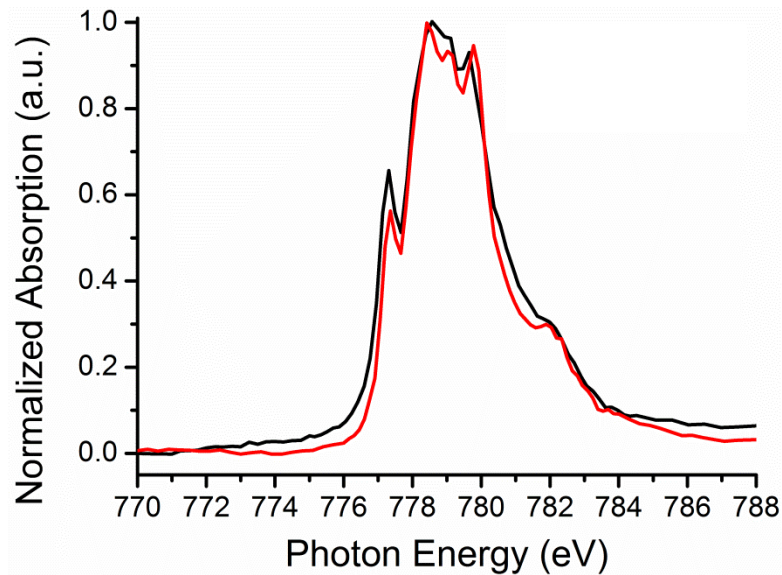


Figure S2: A comparison of the normalized soft X-ray absorption spectra of CoO (black) and CoTiO₃ (red) as measured using STXM.

3. Scanning Transmission Electron Microscopy – Electron Energy Loss Spectroscopy

The complete STEM-EELS data is shown in Figure S3. There is little contrast between Co and TiO₂ in the transmission images, this is one of the drawbacks of normal TEM analysis. The clustering of cobalt nanoparticles in the fresh catalyst is more clearly visible in the cobalt elemental maps (right images). In Figure S3B the formation of cobalt nanoparticles in the crevices around the TiO₂ particles is visible.

In the spent catalyst we see the formation of a layer of cobalt very clearly in the cobalt elemental maps. The thickness of the layer was estimated to be 1 – 2 nm.

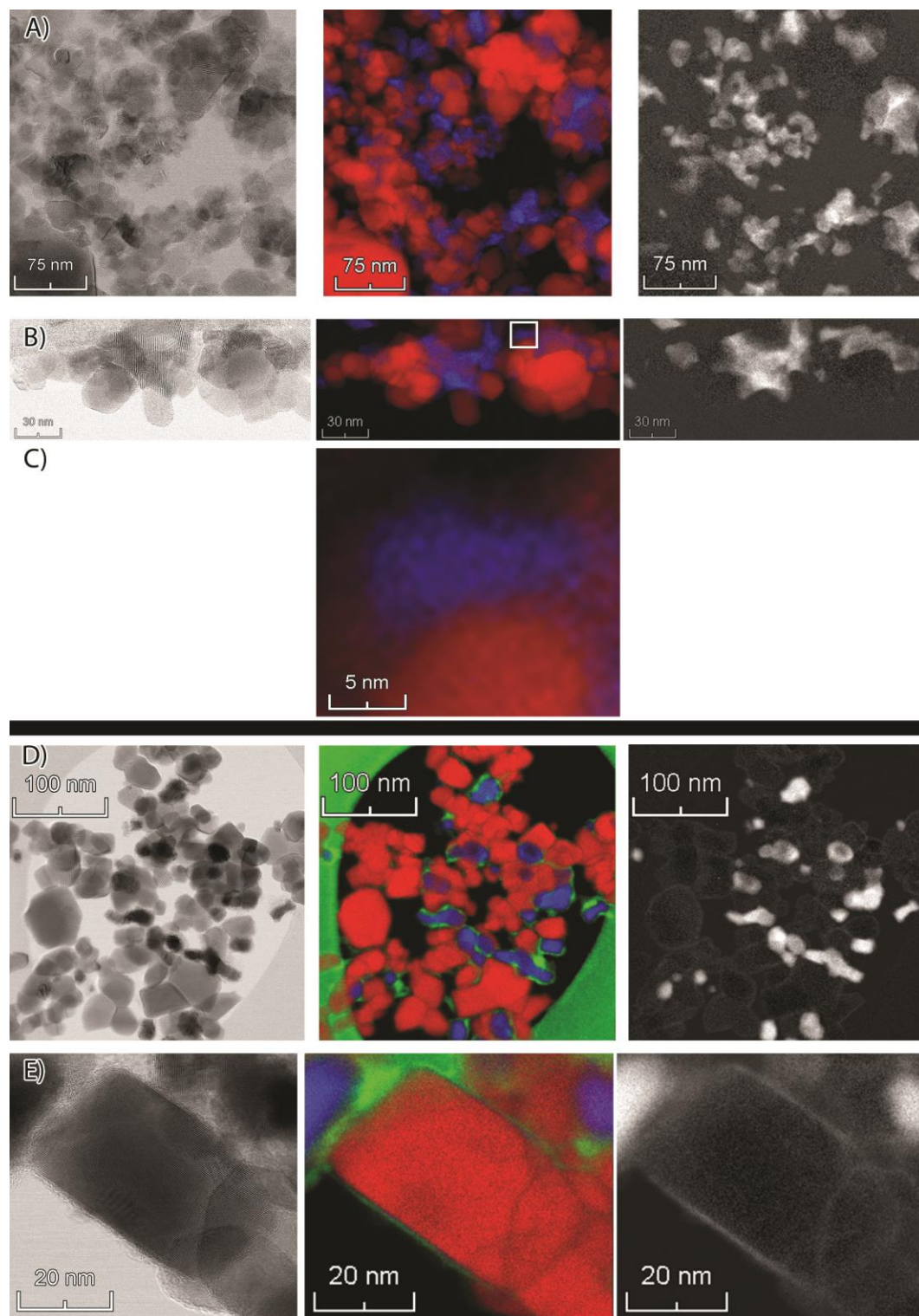


Figure S3. Complete STEM-EELS data. Left images: Bright field STEM images. Middle images: Color-coded elemental maps (red: titanium, blue: cobalt, green: carbon). Right images: cobalt elemental maps. A: fresh catalyst. B: High-resolution image of the fresh catalyst. C: zoomed in image of the region marked in B. D: spent catalyst. E: High-resolution image of the spent catalyst.

4. Statistical Analysis of STEM-EELS Data

To get a more rigorous insight into the distribution of cobalt over the TiO₂ support we made correlation plots for the STEM-EELS data, comparing the intensities (on a scale of 0 – 255) of the cobalt and the titanium elemental maps. The scatter plots for the fresh and spent catalysts are shown in Figure S4.

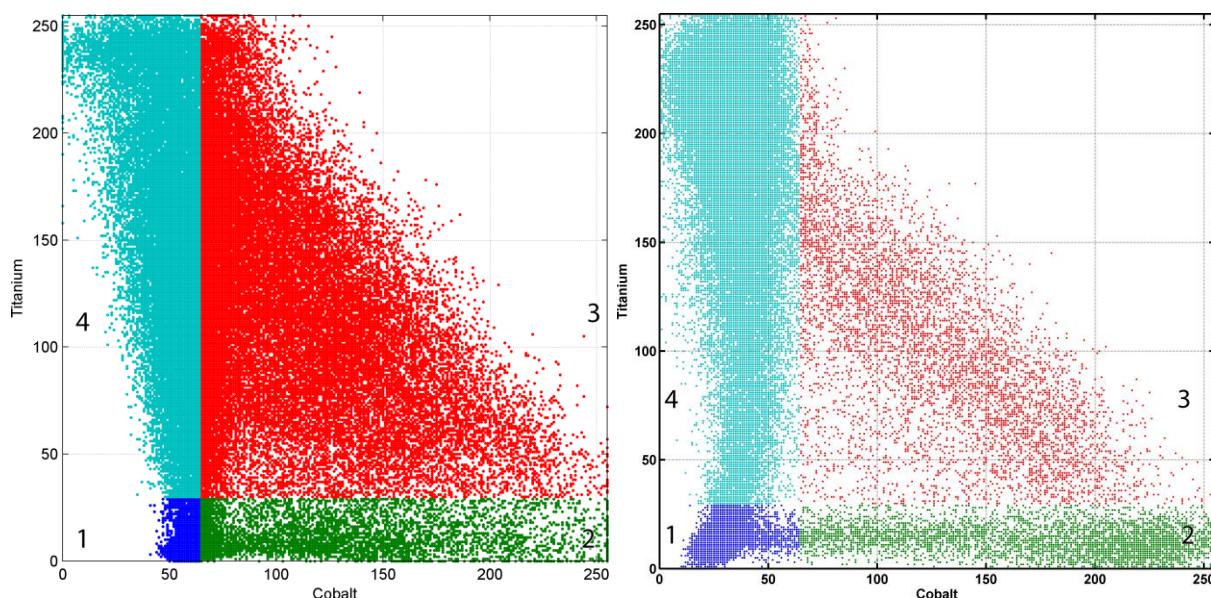


Figure S4: Scatter plot of the STEM-EELS data of the fresh (left) and the spent (right) catalysts. Pixels are plotted according to their contributions of cobalt and titanium. A manual clustering was applied to separate the data into 4 quadrants.

The data were manually segmented into 4 quadrants, numbered 1 – 4. Quadrant 1 is low in contributions from both cobalt and titanium; hence it represents the background of the image. Quadrant 2 is high cobalt but low in titanium. Pixels in this cluster are almost purely cobalt. Quadrant 3 represents pixels that belong to a mixed cobalt/titanium phase. Finally, quadrant 4 is almost purely titanium. The segmented images are shown in Figure S5.

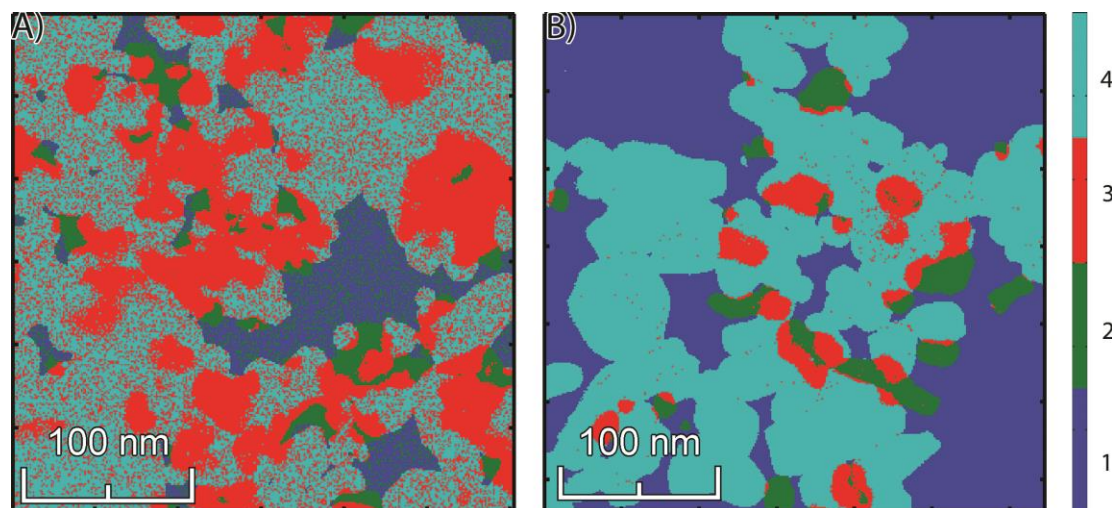


Figure S5: Segmented STEM-EELS images of the fresh (A) and spent (B) catalysts showing the result of the manual clustering into 4 quadrants. The images are color-coded according to the scale on the right.

Comparing the scatter plots for the fresh and the spent catalysts, we see that cobalt and titanium are better separated in the spent catalyst, i.e. more pixels are in quadrant 2 and 4. In case of the fresh catalyst, more pixels are in quadrant 3, i.e. in the mixed phase. Because scatter plots can be hard to interpret quantitatively, we also made histograms of the distribution of all pixels (excluding the background, quadrant 1) over the quadrants, Figure S6. This confirms there are more pixels in quadrant 3 in the fresh catalyst relative to the spent catalyst.

More pixels in quadrant 3 means that the mixed cobalt/titanium phase is more pronounced in the fresh catalyst. This is caused by the relatively large number of cobalt nanoparticles that are (partly) overlapping with titanium particles. These particles can be recognized in the Figure S3A and S3B. On the other hand, the titanium and cobalt are more separated in the spent catalyst. Indeed, there are no such overlapping particles in Figure S3D and S3E.

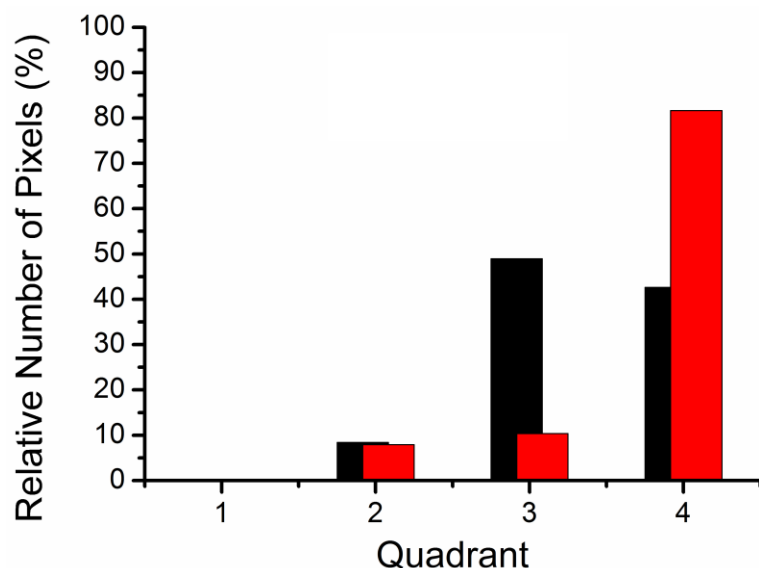


Figure S6: Distribution of pixels over the 4 quadrants shown in Figure S4 for the fresh (black) and the spent (red) catalyst. Quadrant 1 (the background) is excluded from the percentage.

5. Statistical Analysis of STXM Data

We performed a similar analysis for the STXM data. The scatter plots are shown in Figures S7 (correlation plots) and S8 (segmented images). In this case the contributions of the different oxidation states of cobalt were summed to obtain the total cobalt contribution.

In this case we see that the fresh catalyst contains many pixels in a single, but relatively broad cluster. In other words, there is a relatively broad distribution of different ratios between cobalt and titanium. On the other hand, for the spent catalyst almost all pixels are in the background or in a single cluster in quadrant 3. Indeed, this is also what we see in the distribution of pixels over the quadrants (Figure S9). Here we see that in the fresh catalyst there are significant amounts of pixels in quadrants 3 and 4. This means that there are distinct areas where there is a mixed phase, and areas of a high concentration of titanium. This is caused by the clusters of cobalt nanoparticles as discussed in the main text. On the other hand, the spent catalyst almost exclusively contains pixels of a mixed cobalt/titanium phase. From these observations we conclude that cobalt is more homogeneously distributed over the titanium support particles.

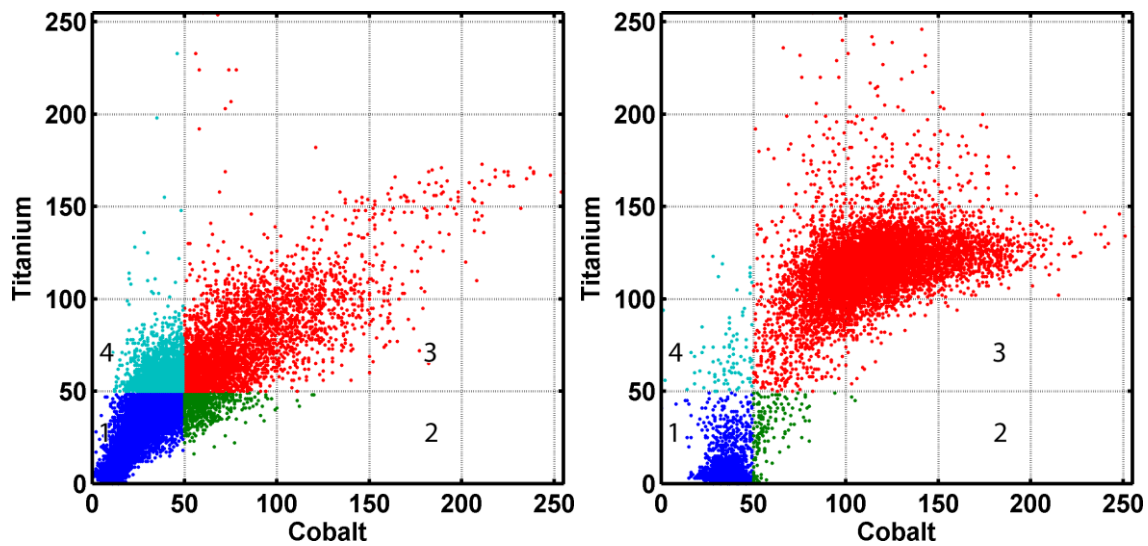


Figure S7: Scatter plot of the STXM data of the fresh (left) and the spent (right) catalysts. Pixels are plotted according to their contributions of cobalt and titanium. A manual clustering was applied to separate the data into 4 quadrants.

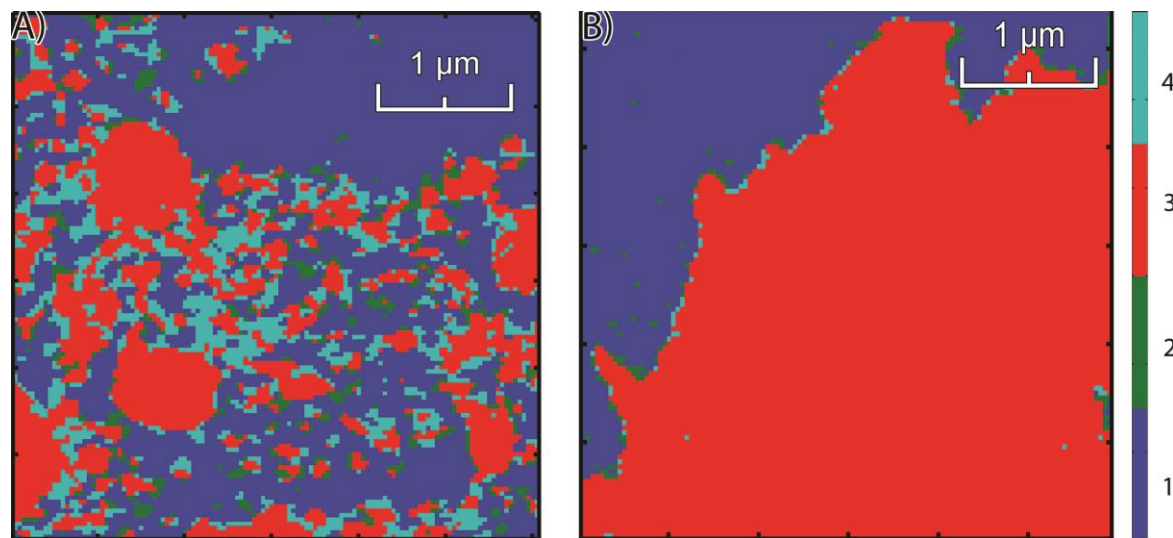


Figure S8: Segmented STXM images of the fresh (A) and spent (B) catalysts showing the result of the manual clustering into 4 quadrants. The images are color-coded according to the scale on the right.

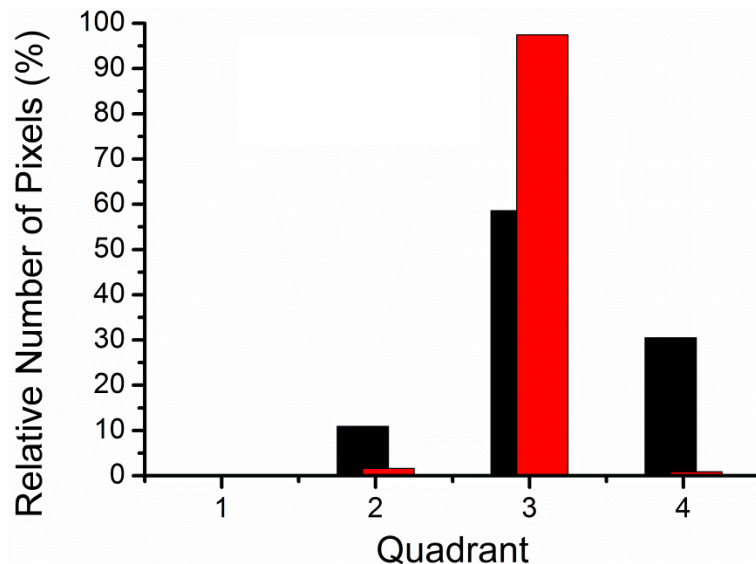


Figure S9: distribution of pixels over the 4 quadrants shown in Figure S7 for the fresh (black) and the spent (red) catalyst. Quadrant 1 (the background) is excluded from the percentage.

6. Statistical Analysis of TXM Data

The TXM data from the main article were also plotted as a correlation plot (Figure S10). In this case we see in the fresh catalyst that all the voxels (as the TXM data are 3-dimensional) are in a single cloud. In contrast, the spent catalyst has all its voxels higher in the scatter plot. The corresponding segmented images are shown in Figure S11.

Due to the huge number of voxels in both TXM datasets it is even more crucial to look at the quantitative distribution of voxels over the quadrants (Figure S12). In case of the fresh catalyst we see that there is a significant number of voxels in quadrants 3 and 4. This means that most of the voxels are in the mixed cobalt/ titanium phase (quadrant 3), but there are also relatively many voxels that are purely titanium (quadrant 4). These are the voxels that contain the clusters that are mentioned in the main text.

On the other hand, we see that for the spent catalyst all voxels are located in quadrant 3, the mixed phase. This illustrates the more homogeneous distribution of cobalt over the titanium support. In other words, the clusters have disappeared during the FTS reaction.

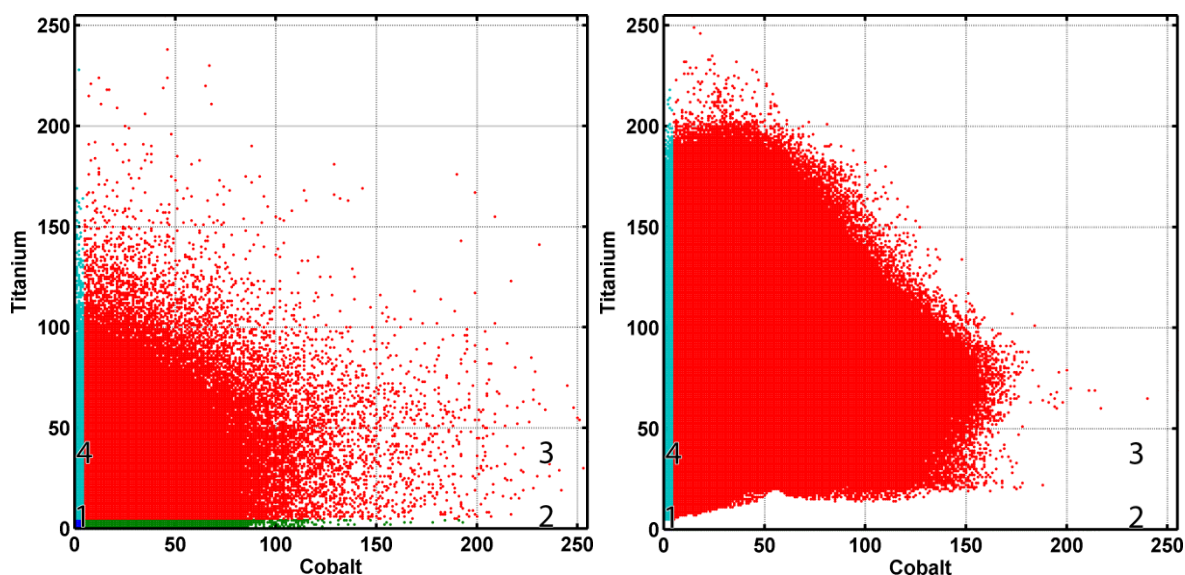


Figure S10: Scatter plot of the TXM data of the fresh (left) and the spent (right) catalysts. Pixels are plotted according to their contributions of cobalt and titanium. A manual clustering was applied to separate the data into 4 quadrants.

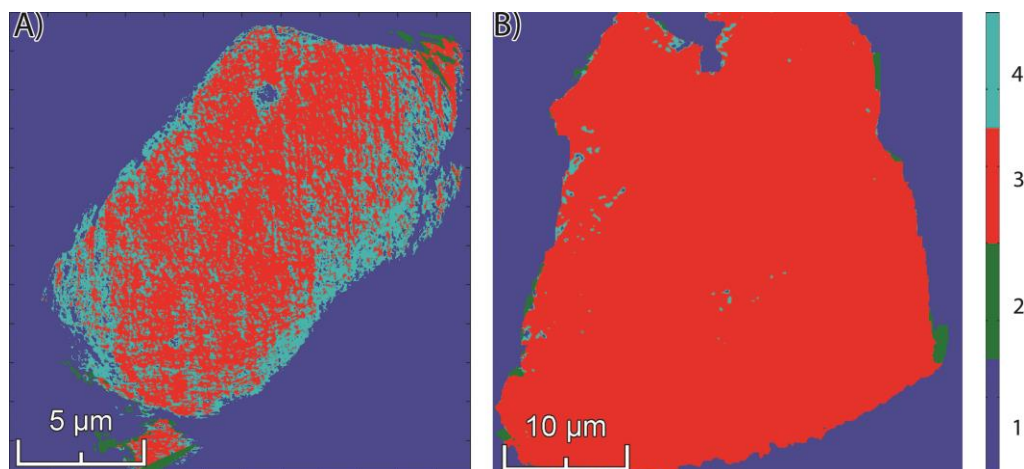


Figure S11: Segmented TXM images of the fresh (A) and spent (B) catalysts showing the result of the manual clustering into 4 quadrants. The images are color-coded according to the scale on the right.

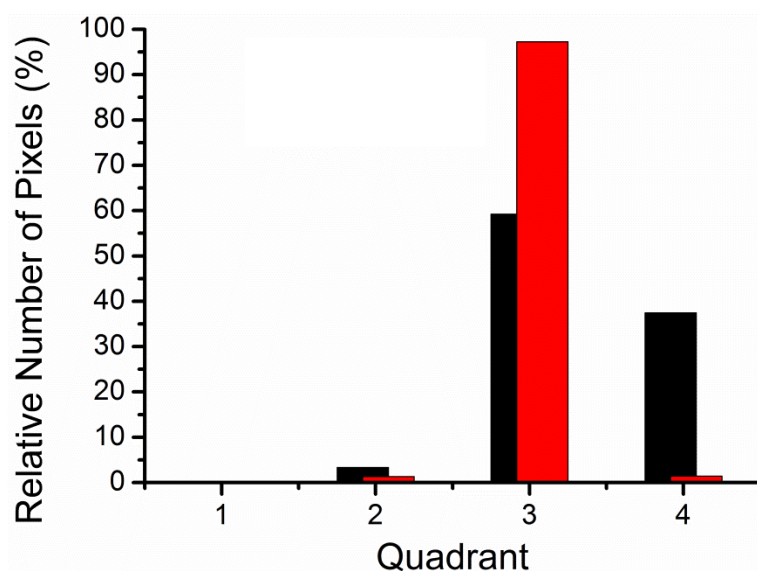


Figure S12: Distribution of pixels over the 4 quadrants shown in Figure S9 for the fresh (black) and the spent (red) catalyst. Quadrant 1 (the background) is excluded from the percentage.

7. In Situ Transmission X-ray Microscopy Data

The spent 15 wt% Co/TiO₂ catalyst was analyzed under reaction conditions in the TXM using a specially designed set-up that was described earlier.^{1,2} A few grains of the sample were loaded into a glass capillary, which was attached with high-temperature epoxy to a holder that allows translation in the *x,y,z* directions, and rotation around the *y*-axis. The sample was first characterized at room temperature under a helium atmosphere. Then, the catalyst was reduced in a flow of hydrogen at a temperature of 350 °C, while TXM X-ray Absorption Near-Edge Spectroscopy (XANES) scans were performed. After about 3 h at this temperature, the temperature was lowered to 250 °C and the gas flow was switched to hydrogen and carbon monoxide in a ratio of 2. Due to the switching of the gas flows, the particle moved inside of the capillary, and a new particle had to be found. The pressure was then increased to 10 bar. TXM XANES scans were performed continuously for about 10 h. The results of these experiments are shown in Figures S13 – S15.

There is a quick and complete reduction (within one XANES scan) to metallic cobalt. During the FTS reaction the catalyst stays metallic, with only small and statistically not significant contributions of oxidized species (CoO or CoTiO₃) to the fits of the averaged spectra. Also in the spatially resolved spectra no significant contributions of oxidized cobalt species can be detected.

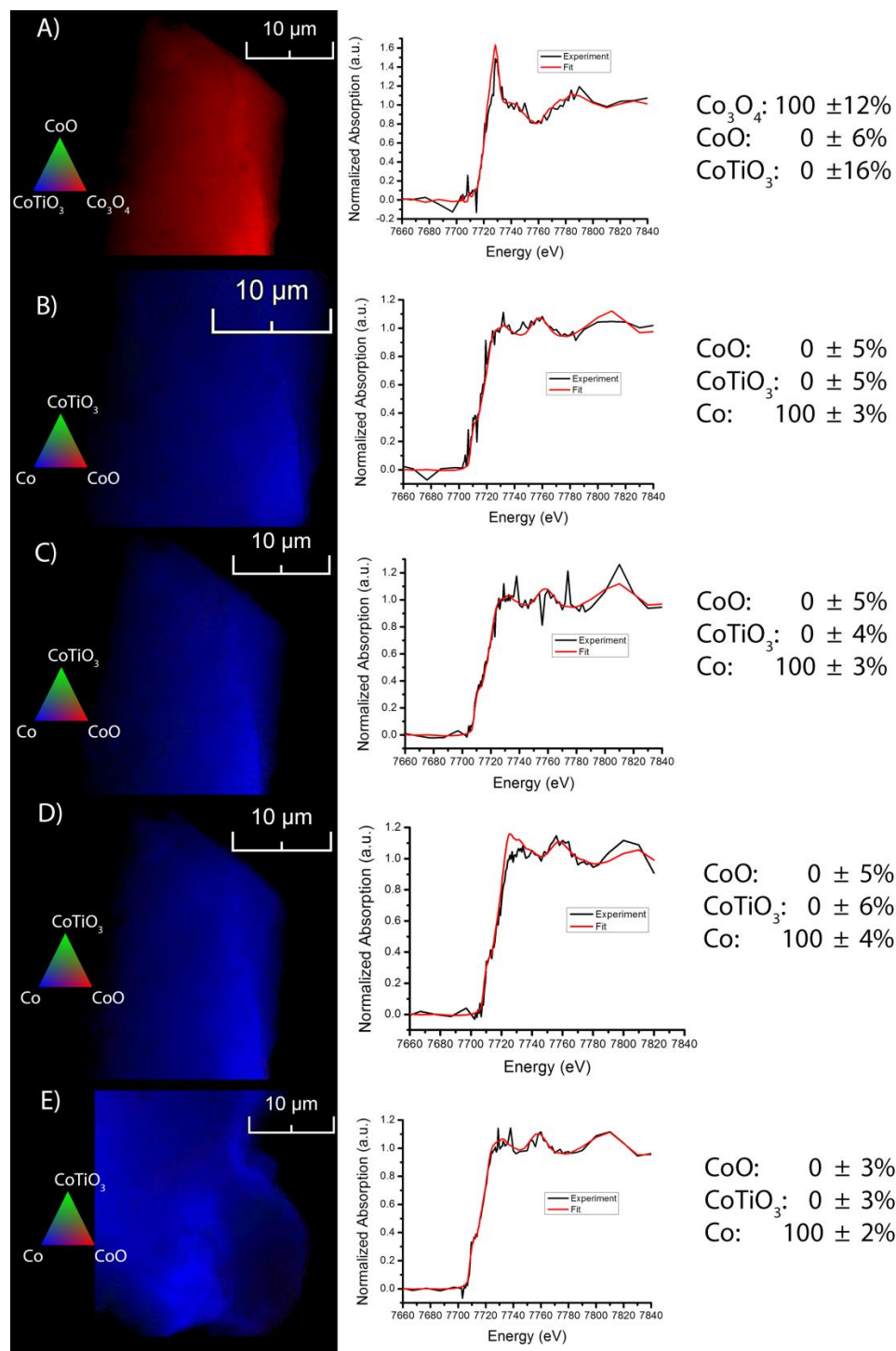


Figure S13: 2-D Transmission X-ray Microscopy images of the spent 15 wt% Co/TiO₂ catalyst particle. Left panel, Chemical maps, middle panel, Average X-ray Absorption Near Edge Spectra (XANES) and right panel, least squares fitting results of the spectra in the middle plane. The data were measured: (A) at room temperature, (B–D) during reduction under H₂ at 350°C after 0 min (B), 45 min (C) and 90 min (D), (E) during Fischer-Tropsch synthesis at 250°C and 10 bar pressure in CO/H₂ in a ratio 1:2 for 0 h on stream. A different particle was measured in (E).

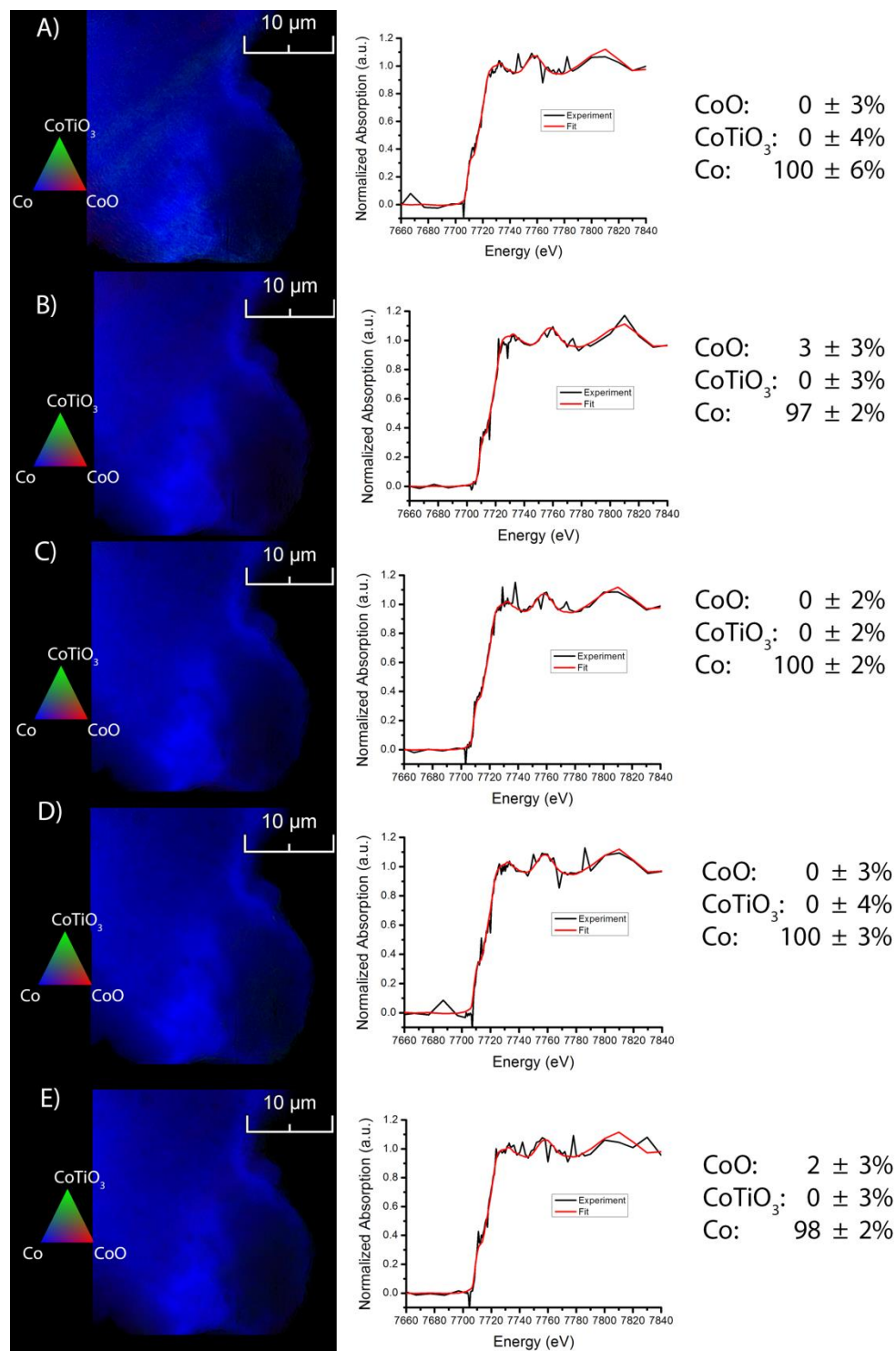


Figure S14: 2-D Transmission X-ray Microscopy images of the spent 15 wt% Co/TiO₂ catalyst particle. Left plane, chemical maps, middle plane, Average X-ray Absorption Near Edge Spectra (XANES) and right plane, least squares fitting results of the spectra in the middle plane. The data were measured during Fischer-Tropsch synthesis at 250°C and 10 bar pressure in CO/H₂ in a ratio 1:2 for 0.8 h (A), 1.6 h (B), 2.4 h (C), 3.2 h (D), 4.0 h (E) on stream.

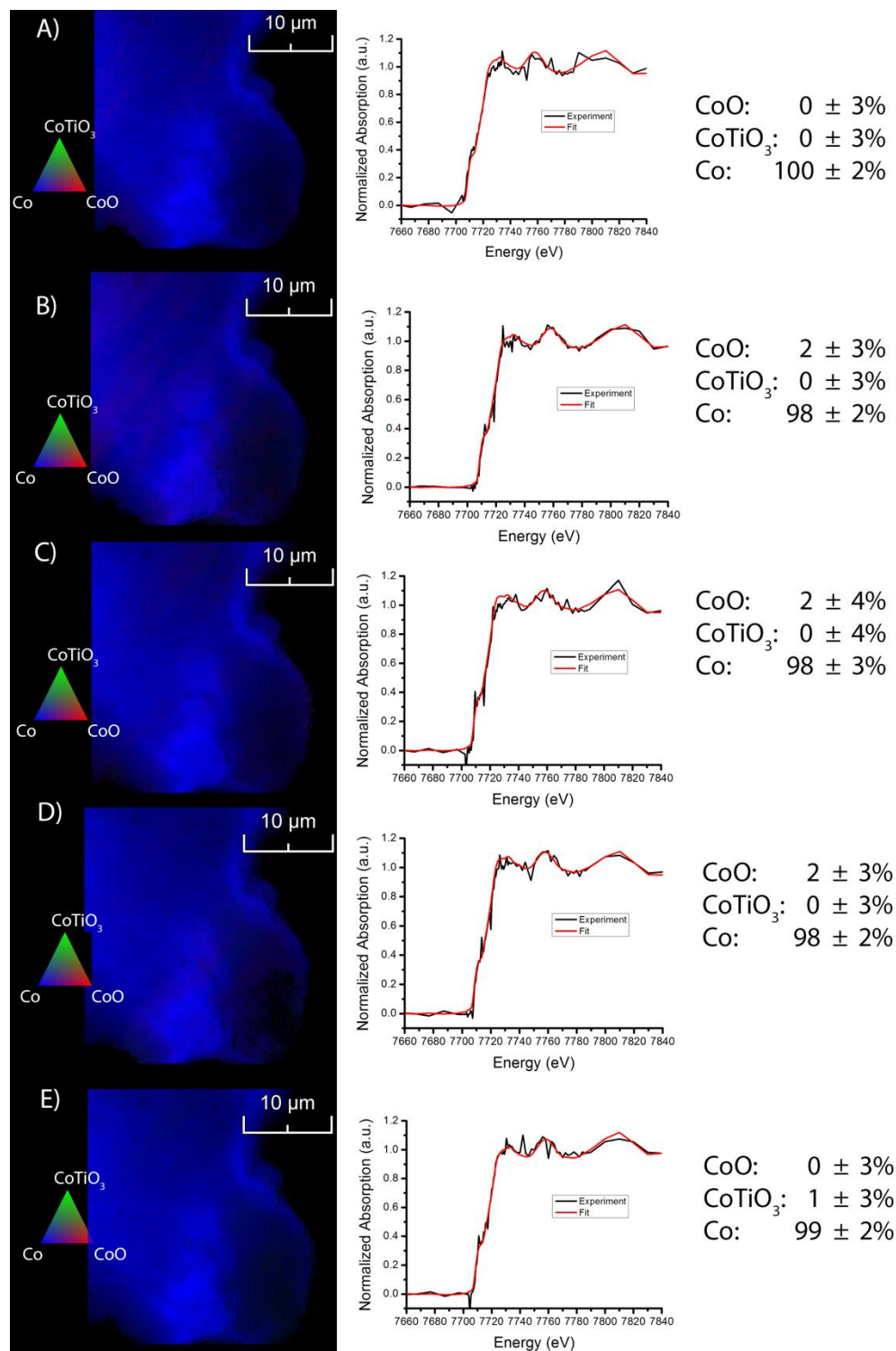


Figure S15: 2-D Transmission X-ray Microscopy images of the spent 15 wt% Co/TiO₂ catalyst particle. Left plane, chemical maps, middle plane, Average X-ray Absorption Near Edge Spectra (XANES) and right plane, least squares fitting results of the spectra in the middle plane. The data were measured during Fischer-Tropsch synthesis at 250°C and 10 bar pressure in CO/H₂ in a ratio 1:2 for 4.8 h (A), 5.6 h (B), 6.3 h (C), 7.1 h (D), 7.9 h (E) on stream.

The above-discussed statistical analysis was also applied to these TXM data (Figures S13–S15), as well as to the in situ TXM data of the fresh catalyst that were published earlier.² However, only the TXM data under FTS conditions were analyzed, i.e. the data collected during the reduction of the catalyst were excluded. We did not find any evidence for Co oxidation. The results are summarized in Figure S16. The percentage of pixels in quadrant 3 (the mixed Co-Ti phase) is plotted in Figure S16A, while the clustered correlation plots for the final in situ measurements are shown in Figures S16B and C. For the fresh catalyst 82% of the pixels are clustered in quadrant 3 on average during the experiment. There is a relatively large variance over time, because of the noise level of the data. The number of pixels in quadrant 3 for the spent catalyst (red line) is significantly higher, ~95% on average. In this case the variance is lower, because the quality of the data is better.

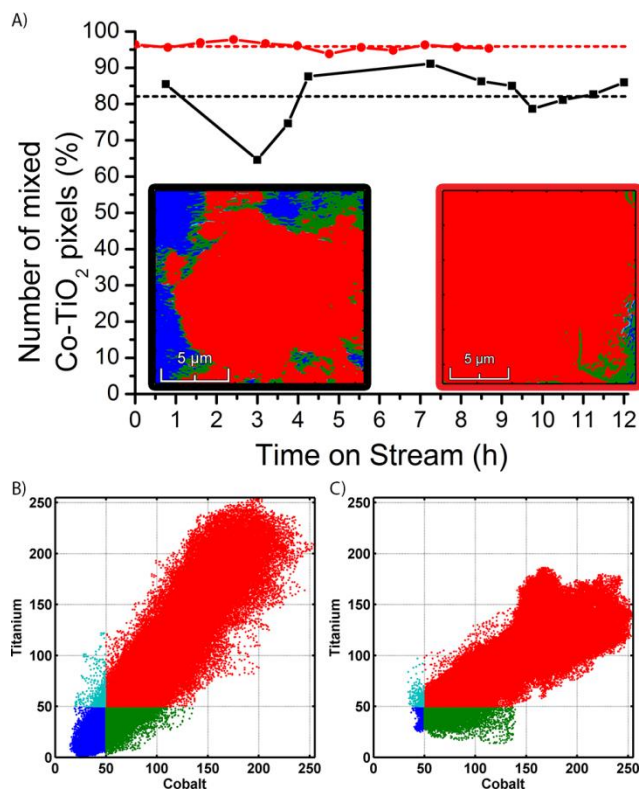


Figure S16: Results of clustering of in situ TXM data for fresh and spent Co/TiO₂ catalyst under FTS conditions (250 °C, 10 bar, 2:1 H₂/CO). A) The number of pixels in quadrant 3 (mixed Co/Ti phase) as a function of time on stream. Fresh and spent catalyst data are plotted in black and red, respectively. The dashed lines indicate the average number of pixels over the time of the experiment. The insets show the clustered images (quadrant 1 in blue, quadrant 2 in green, quadrant 3 in red and quadrant 4 in cyan) of the final in situ experiment for the fresh (left) and spent (right) catalyst. B) Correlation plot of the last time point for the fresh catalyst showing the division of the data into 4 quadrants. C) Correlation plot of the last time point for the spent catalyst.

References

- (1) Gonzalez-Jimenez, I. D.; Cats, K.; Davidian, T.; Ruitenbeek, M.; Meirer, F.; Liu, Y.; Nelson, J.; Andrews, J. C.; Pianetta, P.; de Groot, F. M. F.; Weckhuysen, B. M. *Angew. Chem. Int. Ed.* **2012**, *124*, 12152.
- (2) Cats, K. H.; Gonzalez-Jimenez, I. D.; Liu, Y.; Nelson, J.; van Campen, D.; Meirer, F.; van der Eerden, A. M. J.; de Groot, F. M. F.; Andrews, J. C.; Weckhuysen, B. M. *Chem. Comm.* **2013**, *49*, 4622.